Influence of Mn/Ca ratio in Mn-Ca Coordination Clusters: Synthesis, Structure, and Magnetic Characterisation

AKO, Ayuk M., ANSON, Christopher E., CLÉRAC, Rodolphe, FITZPATRICK, Anthony J. <http://orcid.org/0000-0001-9436-8129>, MÜLLER-BUNZ, Helge, CARTER, Anthony B., MORGAN, Grace G. and POWELL, Annie K.

Citation:

Influence of Mn/Ca ratio in Mn-Ca Coordination Clusters: Synthesis, Structure, and Magnetic Characterisation[‡]

Ayuk M. Ako,[a,b] Christopher E. Anson,[a] Rodolphe Clérac,[c] Anthony J. Fitzpatrick,[b,d] Helge Müller-Bunz,[b] Anthony B. Carter,[b] Grace G. Morgan,[b] and Annie K. Powell*[a,e]

[a] Institute of Inorganic Chemistry, Karlsruhe Institute of Technology, Engesserstrasse 15, 76128 Karlsruhe, Germany.
[b] School of Chemistry, University College Dublin (UCD), Dublin, Ireland.
[c] Université Bordeaux, CNRS, Centre de Recherche Paul Pascal, UMR 5031, 33600 Pessac, France.
[d] Department of Biosciences and Chemistry, Sheffield Hallam University, Sheffield S1 1WB, UK
[e] Institute of Nanotechnology, Karlsruhe Institute of Technology, Hermann von-Helmholtz Platz 1, 76344 Eggenstein-Leopoldshafen, Germany.

[‡] Part of the special issue dedicated to the element manganese, entitled "Manganese: A Tribute to Chemical Diversity".
*Corresponding authors- E-mail: annie.powell@kit.edu

Abstract: Similar reactions of $MnCl_2 \cdot 4H_2O$ and $CaCl_2$ with 2,6-bis(hydroxymethyl)-4-methylphenol gave heterometallic coordination clusters with very different nuclearities, depending on the Mn:Ca ratio used. With a 1:1 ratio, the hexanuclear cluster $[Mn^{III}_3Ca^{II}_3(\mu_3\text{-}Cl(HL^{Me})_6(H_2O)_6]Cl_2 \cdot 6.74H_2O$ (**2**) with a "triangle-in-triangle" topology was obtained. However, a Mn:Ca ratio of 2:1 resulted in $[Mn^{III}_{12}Mn^{II}Ca^{II}_6(\mu_4\text{-}O)_8(\mu_3\text{-}Cl)_{3.7}(\mu_3\text{-}\eta^1\text{-}N_3)_{4.3}(HL^{Me})_{12}(MeCN)_6]Cl_2 \cdot 15MeOH$ (**3**), which corresponds structurally to the replacement by Ca^{2+} of six of the seven Mn^{II} centers in our previously-published cluster $[Mn^{III}_{12}Mn^{II}_7(\mu_4\text{-}O)_8 (\mu_3\text{-}\eta^1\text{-}N_3)_8(HL^{Me})_{12}(MeCN)_6]Cl_2$. Magnetic studies showed that the three Mn^{III} centers in **2** are moderately antiferromagnetically coupled, while the results for **3** allowed an experimental estimate of the $Mn^{III}\text{-}Mn^{III}$ coupling in the original $[Mn_{19}]$ cluster.

Keywords: manganese, calcium, coordination cluster, molecular magnetism

1. Introduction

Manganese-based complexes continue to attract intense research interest because they serve as models for various metalloenzymes[1-4] and can show interesting magnetic properties.[5-7] Along these lines, Mn/Ca compounds are of particular interest because of their

relevance to the oxygen-evolving complex (OEC) within photosystem II (PSII).[8-11] Several studies have demonstrated that the OEC contains a Mn_4CaO_5 core although the exact structure is still unclear, leading to additional interest in Mn/Ca clusters. To this end we and others have reported heterometalic Mn/Ca molecular species, some of which fulfil the details of the nuclearity of the isolated core structure that models the OEC.[12-17] Additionally, it has previously been shown that the OEC requires not only Ca^{II} but also Cl^- for the catalytic cycle to proceed.[18,19]
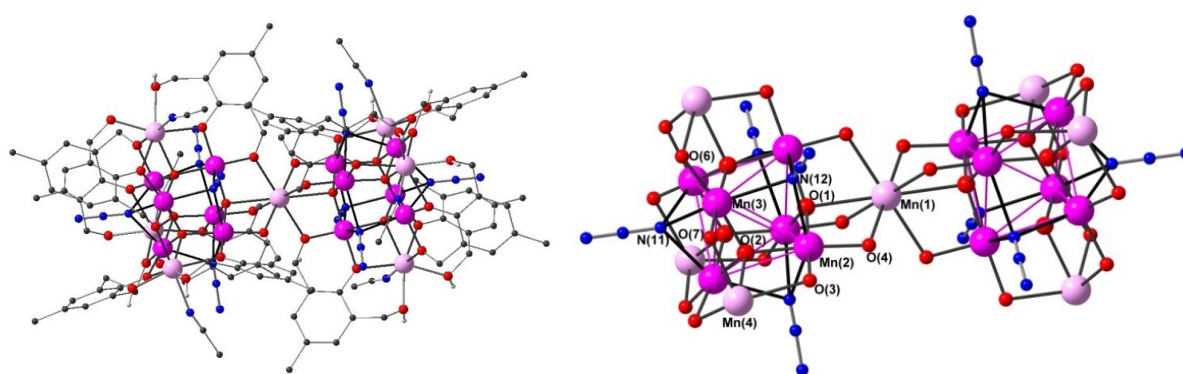
Figure 1. Molecular structure of **1** in the crystal (left) and the metallic core with partial atom numbering scheme (right). Carbon-bound hydrogen atoms, counterions and noncoordinated solvent molecules have been omitted for clarity. Colour code: Mn^{III}, dark pink; Mn^{II}, pale pink; O, red; N, blue.[20]

For some time now, we have been exploring the use of the H_3L^R ligand system based on 2,6-*bis*(hydroxymethyl)-4-R-phenol (R = H, Me, I, F, OMe, SMe) and successfully developed reproducible routes for the syntheses of homometallic $[Mn_{19}]$, complex **1**, (Figure 1) and/or heterobimetallic $Mn_{18}M$ (M = Cd, Sr, Dy, Lu, Y) aggregates.[20-25] The $[Mn_{18}M]$ compounds were obtained through the targeted replacement of the central Mn^{II} in **1** with the heterometal ion, M^{n+}, which could be achieved by the simple addition of the corresponding metal salt to the reaction mixture that afforded **1**. In the synthesis of these $[Mn_{18}M]$ clusters we found that a 2:1 Mn/M ratio resulted in the clean replacement of the central Mn^{II} in **1** by the heterometal M, while increasing the amount of M failed to replace further Mn centres. Considering that the $[Mn_{19}]$ system is completely ferromagnetically coupled to give the

maximum spin ground state of $S_T = 83/2$, a useful goal was to isolate the {Mn^{III}_6} octahedra inscribed within the vertex-sharing supertetrahedron core of **1,** by replacing all the Mn^{II} centres with diamagnetic divalent cations, with a view to evaluate the magnetic behaviour of the two Mn^{III}_6 cores within the structure of **1**. To this end, we deliberately targeted the Ca^{2+} ion because it not only has a similar charge number and size to Mn^{II} but also presents flexibility in coordination preferences, being often found in either seven- or eight-coordinate environments as exhibited by the Mn^{II} centres in **1**. This is in contrast to our previously reported [$Mn_{18}M$] systems, which incorporated heterometal ions M that have a much stronger preference for eight-coordinate environments, and so select cleanly the eight-coordinate central position.[24,25] Moreover, the Ca^{2+} ion is known to be an essential cofactor for the water-splitting reaction in Photosystem II,[17] making Mn/Ca coordination clusters of additional interest.

While site-specific replacement or doping of known systems with heterometal ions is synthetically challenging, it still remains an attractive proposition as it enables a systematic study of the chemical, electronic, and physical properties of the resulting mixed-metal species. Such systems may also present distinctly different architectures and magnetic properties compared with the homometallic analogues. Additionally, there has been only limited use of the H_3L^{Me} (2,6-bis(hydroxymethyl)-4-methylphenol) proligand in mixed-metal chemistry.[24,25] Given that the ligand incorporates a phenolic and two flexible hydroxymethyl groups with scope for various levels of deprotonation, a prediction of any reaction outcome is nearly impossible. This adds a certain appeal given that unpredictable and fascinating species have been isolated from such reactions.[26] The study of these has helped to improve our understanding of the relationship between molecular structure and magnetism. Furthermore, it helps to define design principles required for building new molecules with new and/or enhanced properties.

As an extension of our successful synthetic methodology employed in the synthesis of $[Mn_{18}M]$ coordination clusters we report herein the isolation of a unique hexanuclear heterobimetallic $[Mn^{III}_3Ca^{II}_3]$ coordination cluster (**2**) featuring a μ_3-Cl bridged Mn^{III}_3 triangle inscribed within a triangular Ca^{II}_3 shell, and the aggregate $[Mn^{III}_{12}Mn^{II}Ca_6(\mu_4\text{-}O)_8(\mu_3\text{-}\eta^1\text{-}N_3)_{4.3}(\mu_3\text{-}\eta^1\text{-}Cl)_{3.7}(HL^{Me})_{12} (MeCN)_6]Cl_2 \cdot 15MeOH$ (**3**) (H_3L^{Me} = 2,6-*bis*(hydroxymethyl)-4-methylphenol), in which not only the central eight-coordinate Mn^{II} (Mn1) has been replaced by Ca^{II} but also (on average) five of the six outer seven-coordinate Mn^{II} ions, (Mn4) in **1**, with remarkable retention of the overall core topology.

2. Experimental

2.1 General Procedures

All reactions were carried out under aerobic conditions. Unless otherwise stated all reagents were obtained from commercial sources, and were used as received, without further purification. Elemental analyses (CHN) were performed using an Elementar Vario EL analyzer. FTIR spectra were measured on a Perkin Elmer Spectrum One spectrometer with samples prepared as KBr pellets. *Caution! Although no such tendency was observed during the present work, azide salts are potentially explosive and should be handled with care and in small quantities.*

2.2 X-ray Data Collection and Structure Refinement

Crystal data for **2** were collected at 100 K using an Agilent SuperNova A diffractometer fitted with an Atlas detector and a Mo-microfocus source, while data for **3** were collected at 150 K on a Stoe IPDS II diffractometer, using a Mo-$K\alpha$ rotating-anode source; data were corrected for absorption. The structures were solved by direct methods using SHELXS-97[27] and refined by full matrix least-squares on F^2 for all data using SHELXL.[27, 28] Anisotropic thermal displacement parameters were used for all non-disordered non-hydrogen atoms.

Hydrogen atoms bonded to carbon were added at calculated positions and refined using a riding model. For **2**, the hydrogen atoms of the aquo ligands and of one of the lattice waters were in the difference Fourier map and refined with DFIX geometrical restraints. After convergence they were then refined as rigid groups. The O-H bonds in 3 were restrained to 0.88(4) Å using DFIX. Disordered lattice solvent molecules and counterions which could not be refined satisfactorily using partial atom occupancies and suitable restraints were handled using the SQUEEZE option in PLATON.[29]

The face-bridging ligands in **3** were found to be disordered superpositions of chloride and azide; refinement with appropriate geometrical restraints applied to the azide ligands and similarity restraints to the temperature factors of closely-separated chlorine and nitrogen atoms was straightforward. The relative occupancies of the azide and chloride ligands in the structure were refined, giving overall proportions in agreement with the microanalytical data, and were then fixed in the refinement cycles. The distribution of the six Ca^{2+} ions over the seven M^{II} sites in **3** was determined by comparison of their temperature factors, which depend on whether they are modelled as Mn^{2+} (23 e) or Ca^{2+} (18 e), with those of the central Mn^{III} (which must be pure Mn), followed by refinement of the relative Mn/Ca occupancies. It was found that if the central metal centre M(1) was assigned as Mn, the temperature factor for this atom became high compared with those for the Mn^{III} centres. Refinements of this central atom as a mixture of Mn and Ca all converged with the Ca occupancy not differing significantly from unity, and so this was fixed as 1 (i.e. pure Ca) in subsequent refinements. However, it was also clear that the outer divalent cation sites corresponded to a disordered mixture of Ca and Mn. Refinement as pure Mn gave a temperature factor that was again 40-50% higher than for the Mn^{III} centres, whereas refinement as Ca gave a temperature factor slightly lower than those for Mn^{III}. Comparison with the relative magnitudes of the Mn temperature factors in the original [Mn$_{19}$] (**1**) thus indicated that the outer divalent metal sites in **3** were mostly, but not exclusively,

calcium. Refinements of this cation as a Ca/Mn mixture starting from different relative occupancies generally converged to a situation where the Mn component was in the range 15-20%, and this was fixed at 16.7% ($\frac{1}{6}$), *i.e.* an average of one Mn and five Ca over the six equivalent sites in the molecule as a whole, in the later refinements.

Electron density corresponding to a disordered mixture of the two chloride counterions and ten lattice MeOH was noted at typical hydrogen bonding distances from the twelve ligand O-H groups (O(5) and O(8) and their symmetry equivalents), but these could not be refined satisfactorily. The contributions of the chlorides and the lattice solvent to the scattering factors was therefore calculated using SQUEEZE; per cluster, 305 e were found in 1125 Å^3 and assigned as two chlorides and 15 MeOH (calc. 306 e).[29]

Crystallographic data and structure refinement details for compounds **2** and **3** are summarised in Table 1.

Table 1: Crystal Data for Compounds (2) and (3)

Compound	(2)	(3)
formula	$C_{54}H_{85.48}Ca_3Cl_3Mn_3O_{30.74}$	$C_{135}H_{198}Ca_6Cl_{5.7}Mn_{13}N_{18.9}O_{59}$
Mr	1617.86	4186.48
crystal system	hexagonal	trigonal
space group	$P6_3/m$	$R\overline{3}$
T [K]	100(2)	150(2)
a [Å]	12.9435(2)	21.1271(9)
c [Å]	24.4034(3)	34.8646(19)
V [Å^3]	3540.66(9)	13477.1(11)
Z	2	3
ρ_{calcd} [g/cm^{-3}]	1.518	1.547
λ [Å]	0.71073	0.71073
μ(Mo-Kα) [mm^{-1}]	0.940	1.220
F(000)	1683	6463
reflections collected	63466	33212
unique data	3258	6404
R_{int}	0.0290	0.0383

data with [I>2σ(I)]	3026	4616
parameters/restraints	201 / 0	341 / 18
S on F^2 (all data)	1.084	0.914
wR_2 (all data)	0.11109	0.1250
R_1 (I>2σ(I))	0.0410	0.0456
largest residuals [e Å^{-3}]	+0.69 / −0.46	+0.64 / -0.68

2.3 Magnetic Data Collection

Magnetic susceptibility measurements were performed using a Quantum Design MPMS-XL SQUID magnetometer. This magnetometer works between 1.8 and 400 K for dc applied fields ranging from −7 to 7 T. Ac susceptibility measurements were performed with an oscillating ac field of 3 Oe with a frequency between 1 and 1000 Hz. Consistent dc susceptibility at 0.5 or 0.1 T and in-phase ac susceptibility in zero-dc field have been obtained between 1.85 and 15 K without detection of an out-of-phase ac signal up to 1000 Hz and above 1.85 K. These magnetic measurements were performed on freshly prepared polycrystalline samples (19.2 mg for **2** and 7.5 mg for **3**) sealed in a polyethylene bag (3 × 0.5 × 0.02 cm; typical mass of 10-20 mg). Magnetic data were corrected for the sample holder, and diamagnetic contributions

2.4 Synthesis of [Mn$^{III}_3$Ca$^{II}_3$(μ$_3$-Cl)(HL^{Me})$_6$(H$_2$O)$_6$]Cl$_2$·6.74H$_2$O (2)

Method A: A slurry of MnCl$_2$·4H$_2$O (0.1g, 0.5 mmol), Et$_3$N (0.1 g, 1 mmol) and 2,6-bis(hydroxymethyl)-4-methylphenol (0.14 g, 1 mmol) in 25 mL MeCN and 5 mL MeOH was stirred for 30 minutes at room temperature, then solid CaCl$_2$ (0.055 g, 0.5 mmol) was added in small portions. The resulting mixture was stirred for an additional 1 hour, then heated at reflux for 2 hours to afford a dark brown solution, which was cooled and filtered. Dark red crystals of [Mn$^{III}_3$Ca$^{II}_3$(μ$_3$-Cl)(HL^{Me})$_6$(H$_2$O)$_6$]Cl$_2$·6.74H$_2$O (**2**) were obtained after several days, washed with a small amount of MeCN and dried in air over several days. Yield: 25 % (based on Mn).

Elemental analysis (%) calc. for $C_{54}H_{85.48}O_{30.74}Cl_3Ca_3Mn_3$: C 39.97; H 5.34; found: C 39.71; H 5.53; Selected IR data (KBr pellet, cm^{-1}): 475 (m), 515 (m), 551 (s), 627 (vs), 688 (w), 771 (w), 809 (m), 862 (m), 982 (m), 1020 (m), 1160 (m), 1225 (m), 1254 (s), 1311 (m), 1349 (w), 1471 (vs), 1612 (m), 2834 (m), 2863 (m), 2994 (m), 3356 (s,br).

Method B: A slurry of MnCl$_2$·4H$_2$O (0.1g, 0.5 mmol), CaCl$_2$ (0.055 g, 0.5 mmol), NaSCN (0.15 g, 1.5 mmol), 2,6-bis(hydroxymethyl)-4-methylphenol (0.14 g, 1 mmol) and Et$_3$N (0.1g, 0.1 mmol) in 25 mL MeCN and 5 mL MeOH was stirred for 15 minutes at ambient temperature, then heated at reflux for 2 hours to afford a dark brown solution, which was cooled and filtered. Dark red crystals of (**2**) were obtained after one week, washed with a small amount of MeCN and dried in air over several days. Yield: 46 % (based on Mn). The compound was identified by elemental analysis, IR and X-ray unit cell indexation. The same result was obtained when Ca(NO$_3$)$_2$·4H$_2$O was used as source of Ca^{2+}.

2.5 Synthesis of [Mn$^{III}_{12}$Mn^{II}Ca$^{II}_6$(μ_4-O)$_8$(μ_3-Cl)$_{3.7}$(μ_3-η^1-N$_3$)$_{4.3}$(HL^{Me})$_{12}$(MeCN)$_6$]Cl$_2$·15MeOH (3)

A slurry of MnCl$_2$·4H$_2$O (0.4g, 2 mmol), NaN$_3$ (0.2 g, 3 mmol), NaO$_2$CMe·3H$_2$O (0.28 g, 2 mmol) and 2,6-bis(hydroxymethyl)-4-methylphenol (1.02 g, 6 mmol) in 25 mL MeCN and 5 mL MeOH was stirred for 30 minutes at room temperature, then a solution of Ca(NO$_3$)$_2$·4H$_2$O (0.24 g, 1.00 mmol) in 5 mL of MeCN was added. The resulting mixture was stirred for an additional 1 hour, then heated at reflux for 2 h to afford a dark brown solution, which was cooled and filtered. Dark red crystals of [Mn$^{III}_{12}$Mn^{II}Ca$^{II}_6$(μ_4-O)$_8$(μ_3-Cl)$_{3.7}$(μ_3-η^1-N$_3$)$_{4.3}$(HL^1)$_{12}$(MeCN)$_6$]Cl$_2$·15MeOH (**3**) were obtained after a few days, washed with a small amount of MeCN and dried in air over several days. Yield: 30 % (based on Mn). Elemental analysis (%) calc. for $C_{120}H_{202}Ca_6Cl_{5.7}Mn_{13}N_{18.9}O_{76}$ (corresponds to replacement of all lattice MeOH by atmospheric water): C 33.66; H 4.75; N 6.18; found: C 33.62; H 4.53; N 6.25.

Selected IR data (KBr pellet, cm^{-1}): 418 (w), 475 (m), 515 (m), 551 (s), 627 (vs), 688 (w), 771 (w), 809 (m), 862 (m), 899 (w), 947 (w), 982 (m), 1028 (m), 1160 (m), 1225 (m), 1254 (s), 1311 (m), 1349 (w), 1471 (vs), 1563 (w), 1612 (m), 2065 (vs), 2834 (m), 2863 (m), 2998 (m), 3355 (s,br).

3. Results and Discussion

As part of our research program into the synthetic manipulation of the [Mn$_{19}$] scaffold of the [Mn$_{19}$] aggregate [Mn$^{III}_{12}$Mn$^{II}_7$(μ_4-O)$_8$(μ_3-η^1-N$_3$)$_8$(HL^{Me})$_{12}$(MeCN)$_6$] Cl$_2$·10MeOH·MeCN (**1**) with a large ground spin state S_T = 83/2,[20] we reported the incorporation of heterometals (M = Dy, Sr, Cd, Lu, Y) into the system to probe the contribution of these to anisotropy and interaction between the high magnetic Mn$_9$ units.[24,25] Considering that the original [Mn$_{19}$] consists of six 7-coordinate and one 8-coordinate Mn^{II} atoms, and given that Ca^{II} presents a flexibility in coordination preferences, being often found in either seven- or eight-coordinate environments, we postulated that it may be possible to selectively replace some or all the Mn^{II} centres in **1** with diamagnetic Ca^{II} ions with the conservation of the core topology and by so doing exclusively probe the magnetic contribution of the octahedral Mn^{III} centres in the [Mn$_{19}$] system. Indeed, such targeted replacement should be possible considering the similarity in the seven and eight-coordinate effective ionic radii of Mn(II) (1.04, 1.10 Å) and Ca(II) (1.06, 1.12 Å), respectively.[30] Selective incorporation of the Ca^{II} ions into the Mn^{II} sites of the [Mn$_{19}$] system should be consistent with geometric and electronic (charge) matching of the Mn^{II} with Ca^{II}. While this is theoretically feasible, the main challenge is to design a synthetic route to experimentally achieve the theoretical prediction, given that the directed synthesis of high-nuclearity ccoordination clusters in which the core has a specified structural topology remains a very challenging synthetic goal.

We began this study by first attempting to synthesise the $[Mn^{III}_{12}Ca^{II}_7]$ analogue in which all the seven Mn^{II} in **1** are replaced by Ca^{II}. To this end, we initially employed a slight modification of the already established synthetic protocol that was used to obtain the $Mn_{18}M$ compounds. The reaction of $MnCl_2·4H_2O$ and $CaCl_2$ (1:1 stochiometric ratio instead of 2:1 Mn/M ratio employed for $Mn_{18}M$ species) with 2,6-bis(hydroxymethyl)-4-methylphenol (H_3L^{Me}) in the presence of Et_3N in MeCN/MeOH (5:1, v/v) under reflux conditions instead afforded the coordination cluster $[Mn^{III}_3Ca^{II}_3(\mu_3\text{-}Cl)(HL^{Me})_6(H_2O)_6]Cl_2·6.74H_2O$ (**2**) with a 25 % yield. It was found that the addition of NaN_3, a typical component in our syntheses of $Mn_{18}M$ clusters, was here not necessary and could be omitted; however, the synthesis of **2** could be optimised by introducing NaSCN into the reaction mixture, nearly doubling the yield (46 %, based on Mn). At this stage it is unclear why the yield is improved since the thiocyanate is not incorporated into the structure. We speculate that the thiocyanate increases the basicity of the reaction mixture. The IR spectrum of **2** shows a strong absorption in the region 3200-3500 cm^{-1}, consistent with the presence of water and the elemental analysis is consistent with **2**·$4H_2O$. When a similar reaction was carried out in strict analogy to our previous synthetic method for the $Mn_{18}M$ coordination clusters [24,25] using $Ca(NO_3)_2·4H_2O$ or $CaCl_2$ as source of Ca in a 2:1 Mn/Ca ratio, the coordination cluster $[Mn^{III}_{12}Mn^{II}Ca^{II}_6(\mu_4\text{-}O)_8(\mu_3\text{-}Cl)_{3.7}(\mu_3\text{-}\eta^1\text{-}N_3)_{4.3}(HL^1)_{12}(MeCN)_6]Cl_2·15MeOH$ (**3**) was obtained, which is close to the target compound. All further attempts to obtain the desired compound $[Mn^{III}_{12}Ca^{II}_7]$ in which all seven of the Mn^{II} in **1** have been replaced by Ca^{2+} by adjusting the Mn:Ca ratio were unsuccessful. However, these results indicate that the reaction involving Ca as hetero metal is indeed sensitive to the Mn/Ca ratio employed in the reaction. This is contrary to our previous observation with other heterometals where optimised yields of the corresponding $Mn_{18}M$ molecular species were obtained strictly for Mn/M metal ratio of 2:1.[24,25] Increasing the amount of heterometal in

the reaction mixture did not alter the Mn/M ratio in the final product nor the topology of the resulting species as observed in compound **2**.

3.1 Structural Description of coordination clusters (2) and (3)

Single crystal X-ray diffraction revealed that compound **2** crystallises in the hexagonal space group $P6_3/m$ with $Z = 2$ and contains hexanuclear heterometallic $[Ca^{II}_3(\mu_3\text{-}Cl)Mn^{III}_3(HL^{Me})_6(H_2O)_6]^{2+}$ cation (Figure 2).
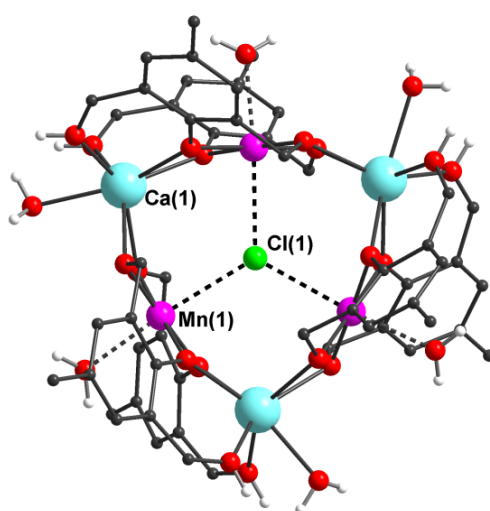
Figure 2. Molecular structure of **2** in the crystal with disorder neglected, with Mn^III Jahn-Teller axes represented with dashed bonds. Carbon-bound hydrogen atoms, counterions and noncoordinated solvent molecules omitted for clarity. Colour code: Mn^III, purple; Ca, pale blue; Cl green, yellow, O red, N blue, C dark grey, H, white.

The structure of **2** consists of a planar μ_3-Cl bridged triangular Mn^III_3 unit inscribed within a trinuclear triangular Ca^II shell. The molecule has crystallographic $\bar{6}$ site symmetry, with the asymmetric unit containing one half Mn^III, one half Ca^II ion, one full HL^Me ligand, two half water ligands (one coordinated to the Mn^III and one to the Ca^II ion), and a one-sixth μ_3-chloride on the $2c$ ($\bar{6}$) special position. Charge balance is provided by a one-sixth chloride disordered either side of the $2d$ ($\bar{6}$) special position and a further chloride disordered against lattice waters over six equivalent positions. The Mn-Cl bond length is 2.7130(3) Å. The Mn^III

and Ca^{II} centres are bridged by deprotonated μ-phenoxo and μ-alkoxo oxygen atoms of the HL^{Me} ligands. Each Mn^{III} ion is in a distorted ClO_5 octahedral coordination environment, comprising the central μ-Cl atom, four oxygen atoms from two HL^{Me} ligands and a water ligand *trans* to the chloride. The Ca centres have an O_7 coordination enviroment, comprising two phenoxo, two alkoxo and two alcohol oxygens from four ligands, with the final oxygen from a water ligand. The Mn⋯Mn and Ca⋯Ca distances are 4.6990(5) Å and 6.4259(9) Å, respectively. The M-O bond lengths to ligand O_{phenol} are 1.9173(13) and 2.3733(14) for M = Mn and Ca, respectively. The Mn^{III} oxidation state and the ligand protonation level were established by bond valence sum (BVS) calculations,[31] charge considerations, and the presence of Mn^{III} Jahn-Teller elongations along the Cl-Mn-OH_2 axes (Figure 2). Note that in **2** each Ca and Mn centre is coordinated by a water molecule. Many proposed mechanisms of water oxidation invoke the coordination of at least one of the substrate water molecules to a Mn centre with a second substrate water thought to bind at Ca,[30-32] which likely serves as a non-redox active Lewis acid for the reaction.[35]

It is noteworthy that the Mn:Ca (3:3) ratio in **2** is consistent with the 1:1 stoichiometric amounts of the metal salts employed in the reaction. This is in contrast to the $Mn_{18}M$ coordination clusters we previously reported, that required a 2:1 Mn:M ratio.[24,25]

Given the critical role of the chloride ion in assembling the structure of the $[Mn^{III}_3Ca^{II}_3]$ coordination cluster, we explored the possibility of substituting the chloride for bromide. The reaction of H_3L^{Me} with $MnBr_2 \cdot 4H_2O$ and $CaBr_2$ in the presence of Et_3N as base in MeCN/MeOH (5:1, v/v) unexpectedly afforded a $[Mn_{19}]$ aggregate, analogous to our reported $[Mn_{19}(O)_8(HL^{Me})_{12}(\mu_3\text{-}Br)_8(MeCN)_6]Br_2 \cdot 16H_2O \cdot 11MeOH$.[23] From this result it can be concluded that the formation of **2** is only possible with Cl^- ion. The structural framework of **2** would have to undergo an expansion upon substitution of the larger Br^- (ionic radius = 1.96 Å)

for Cl- (ionic radius = 1.81 Å) and hence a breakdown of the heterometallic cores topology, probably accounting for the complete absence of Ca in the isolated compound.

Discrete and polymeric oxide-centered triangular $[M_3O(O_2CR)_6L_3]^{n+}$ complexes and/or aggregated triangular $\{Mn_3O\}$ units as well as heterometallic $\{Mn_2MO\}$ or $\{Fe_2MO\}$ (M = transition metal) have been reported for other transition metals.[36-40] A Mn_8 helicate complex featuring two μ_3-Cl bridged Mn^{II}_3 scalene triangles in which the Cl atom deviates slightly from the Mn_3 plane has been reported.[41] Moreover, Christou et al. have reported a near-equilateral Mn^{III}_3 triangle capped by μ_3-O^{2-} ion derived from the H_3L^{Me} proligand.[40] Indeed, examples of carboxylate-free, planar and symmetric $\{Mn^{III}_3(\mu_3\text{-}X)\}$ complexes are scarce. Compound **2** thus joins the limited group of this structural type[42] and to our knowledge is the first example of a structurally characterised mixed-metal species of the system incorporating a Ca^{II}_3 triangle.

The topology and disposition of the heterometals in **2** is quite appealing. The ability of the closed-shell chloride ion to mediate magnetic superexchange between isolated metal ions in this motif can be gauged. There is also the question of what effect the proximity of the diamagnetic Ca^{II} ions may have on the magnetic interaction within the Mn^{III}_3 triangle. We have noticed in our previous work that diamagnetic ions are capable of transmitting, albeit weakly, magnetic information between the 3d centers.[25,44]

Compound **3** crystallises in the trigonal space group *R-3* with *Z* = 3, isotypically to the previously reported $[Mn_{19}]$ and $[Mn_{18}M]$ coordination clusters (Figure 3).[20-25] The metallic content of **3** however differs from that of the previously reported $[Mn_{18}M]$ compounds, in that in addition to the clean replacement of the central eight-coordinate Mn^{II} by Ca^{2+}, five of the six "outer" seven-coordinate Mn^{II} ions have been replaced by Ca^{2+} ions, figure 3. Ca^{2+} and Mn^{2+} differ by only five electrons (18 and 23, respectively) and coordination numbers of both seven and eight are both common for Ca^{2+}.
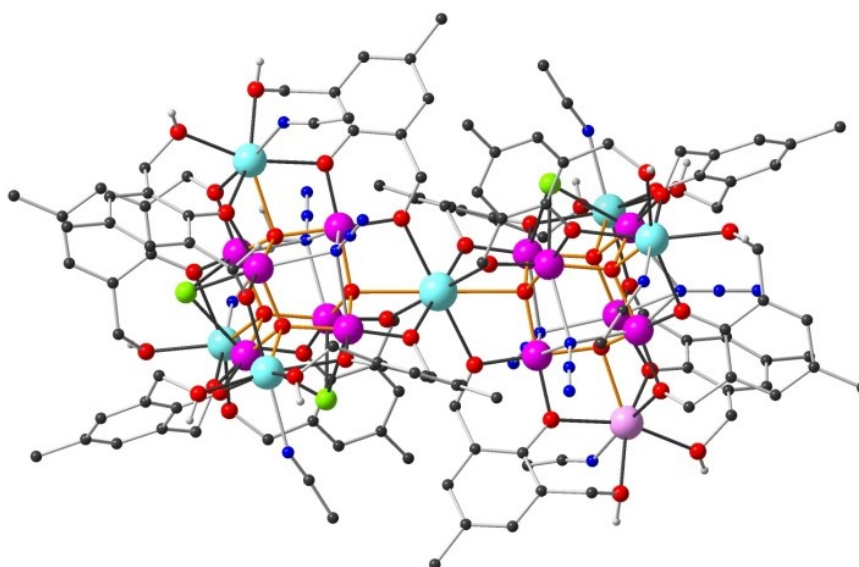
Figure 3. Molecular structure of **3** in the crystal. Organic H atoms, counterions and lattice solvent molecules have been omitted for clarity. Only one of the possible distributions of disordered azide and chloride ligands is shown; similarly the Mn^{II} cation is only shown in one of the six equivalent sites. Colour code: Mn^{III} purple, Mn^{II} pink, Ca pale blue, Cl green, yellow, O red, N blue, C dark grey.

During refinement of the structure, it was found that the central metal centre could be correctly assigned as pure calcium and that the outer divalent metal ions were predominantly but not exclusively calcium. More details were given in the experimental section. Refinement with the central metal as Ca(1), and the outer centres assigned as 83.3% Ca and 16.7% Mn, *i.e.* an overall formulation of $Mn^{III}_6Mn^{II}Ca_6$ for the core, with a single Mn^{II} occupying one of the outer sites as a statistical distribution (given the symmetry of the molecule) was found to be most appropriate. The final U_{eq} values for Ca(1), Mn(1), Mn(2) and Ca/Mn(3) were 0.0383(3), 0.03463(14), 0.03370(14) and 0.03815(16) $Å^2$, respectively, with their trend in good agreement with that for the values found in **1**. The Ca(1)-O(1) and Ca(1)-O(4) bond lengths in **3**, 2.582(3) and 2.4310(19) Å, respectively, are significantly longer than the corresponding Mn(1)-O bond lengths in **1**, 2.507(3) and 2.4449(19) Å, respectively.[20] The Ca(3)-O bond lengths in **3**, 2.2845(18)-2.3752(19) Å, are also longer than the Mn(4)-O distances in **1**, 2.1868(19)-2.3607(19) Å, while the difference between Ca(3)-N(1) in **3** and Mn(4)-N(1) in **1**, 2.402(3) and 2.275(3) Å, respectively, is noteworthy. The oxidation states of Mn(1) and Mn(2) in **3** were

confirmed as Mn[III] by Bond Valence Sum calculations,[31] with calculated valences 2.96 and 2.91, respectively. The Mn[III]$_6$Mn[II]Ca$_6$ composition was also found to be consistent with the magnetic data for **2** (*vide infra*). Such disordering of heterometal ions over various sites in a given system has previously been reported by the Winpenny group.[45] As previously observed, the chloride counterions in **3** accept hydrogen bonds from the alcohol –OH groups of the organic ligands, and are disordered against lattice methanols. Compound **3** represents the highest nuclearity Mn/Ca coordination cluster reported to date and may prove to have interesting catalytic properties which will be the subject of a future study. It is also worth noting that the replacement of essentially all the Mn^{2+} ions in **1** with Ca^{2+}, with remarkable retention of core topology, as observed in the cluster compound **3** is rare and represents a significant result. Few examples exist whereby heterometallic species have been obtained through this method[45-48] and in most cases, the attempted substitution of a specific metal site usually leads to structural changes,[45,46] as observed in compound **2**.

3.2 Magnetic Properties of (2) and (3)

The magnetic properties of a polycrystalline sample of **2** were measured between 4 to 300 K at 0.5 T as shown in figure 4. At 300 K, the χT product (χ being the molar magnetic susceptibility) is equal to 7.50 cm^3 K mol^{-1}, which is significantly lower than the expected Curie value (9 cm^3 K mol^{-1} with $g = 2$) for three Mn(III) $S = 2$ magnetic sites. This low χT value is indeed the consequence of antiferromagnetic interactions between Mn(III) spins, which are clearly detected on lowering the temperature by the decrease of the χT product (which reaches 1.0 cm^3 K mol^{-1} at 4 K). Taking into account the trigonal symmetry of the molecular structure of [Mn[III]$_3$Ca[II]$_3$(μ_3-Cl)(HL^{Me})$_6$(H$_2$O)$_6$]Cl$_2$·6.74H$_2$O, the following Heisenberg spin Hamiltonian, $\boldsymbol{H} = -2J\,(\boldsymbol{S}_1\!\cdot\!\boldsymbol{S}_2 + \boldsymbol{S}_2\!\cdot\!\boldsymbol{S}_3 + \boldsymbol{S}_1\!\cdot\!\boldsymbol{S}_3)$, was considered with $S_i = 2$ for the Mn(III) metal ions. Application of the van Vleck equation[50] to Kambe's vector coupling

scheme[51] allows one to determine an analytical expression of the magnetic susceptibility in the low field approximation and to fit the experimental data, as shown in Figure 4.
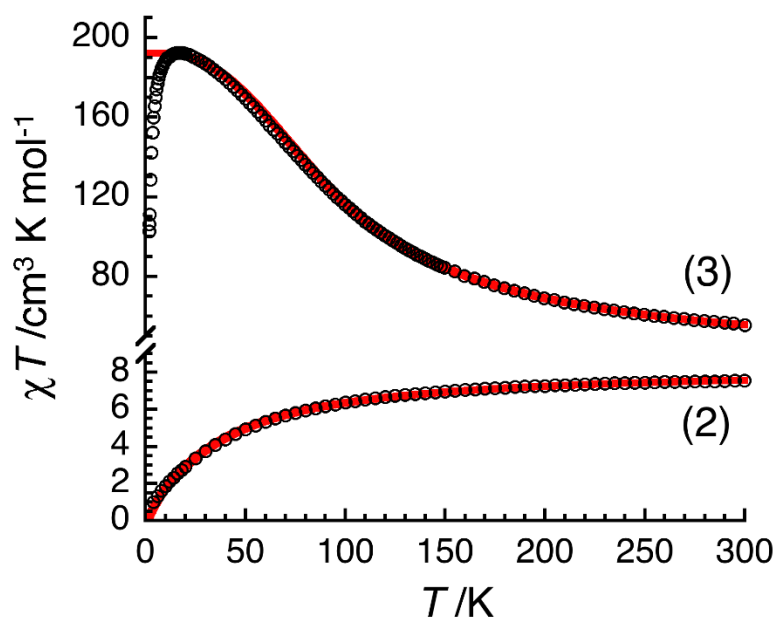

Figure 4. Temperature dependence of the χT product (where χ is the molar magnetic susceptibility that equals M/H per complex) collected in an applied dc magnetic field of 0.05 T for **2** and 0.1 T for **3**. The solid red lines are the best fits to the model described in the text.

Over the whole temperature range, the experimental data are perfectly reproduced with J/k_B = -3.3(1) K and g = 1.92(5). This result shows that there is a moderate antiferromagnetic exchange between the magnetic manganese centres mediated by the central μ_3-Cl anion and/or the diamagnetic O_2CaO_2 bridges. No slow relaxation of the magnetisation, i.e. Single-Molecule Magnet properties, was observed by ac susceptibility measurements, at least in the instrumental measurement window (above 2 K and with ac frequencies up to 1000 Hz). Lower temperature magnetic studies, as well as theoretical calculations would be required to fully rationalize the origin of the magnetic exchange properties of **2**. In the now well-known triangular Dy$_3$ molecular coordination cluster, the anisotropy axes of the three Dy^{III} cations are arranged tangentially to the triangle resulting in a toroidal non-magnetic ground state.[52] By contrast,

the Jahn-teller axes of the Mn(III) centres in **2** are arranged radially to the triangle, and (if the anisotropy were strong enough) this would lead to a different unusual spin structure.

The magnetic properties of $[Mn^{III}_{12}Mn^{II}Ca^{II}_6(\mu_4\text{-}O)_8(\mu_3\text{-}Cl)_{3.7}(\mu_3\text{-}\eta^1\text{-}N_3)_{4.3}(HL^1)_{12}(MeCN)_6]Cl_2\cdot10MeOH\cdot MeCN$ (**3**) were measured on a polycrystalline sample. The temperature dependence of the susceptibility and field dependence of the magnetisation for **3** are shown as a χT vs. T plot in Figure 4 and as M vs. H and M vs. H/T plots in Figure 5, respectively. The experimental χT product is 55.6 cm³K mol⁻¹ at 300 K, which is higher than the expected value (40.375 cm³K/mol) for non-interacting metal ion spins including twelve Mn^{III} ions ($S = 2$, $C = 3.0$ cm³ K mol⁻¹) and one Mn^{II} ion ($S = 5/2$, $C = 4.375$ cm³ K mol⁻¹). In contrast to **2**, this high χT value is induced by the presence of dominant ferromagnetic interactions in **3**, which are clearly observed by the increase of the χT product when the temperature is lowered. Under an applied field of 0.1 T, it increases continuously to reach a maximum of 192 cm³ K mol⁻¹ at 17 K. Below this temperature, χT then rapidly drops, reaching 102.7 cm³ K mol⁻¹ at 1.85 K, as was similarly observed for the $[Mn_{18}M]$ (M = Sr, Y, Lu) compounds.[25] This low temperature behaviour is a combined effect of (i) the fast field saturation of the magnetization, even at low fields, as units with large ground state spins are present in this system (*vide infra*), (ii) weak intra- and/or intermolecular antiferromagnetic interactions and/or (iii) the magnetic anisotropy intrinsic to the Mn^{III} metal ions.
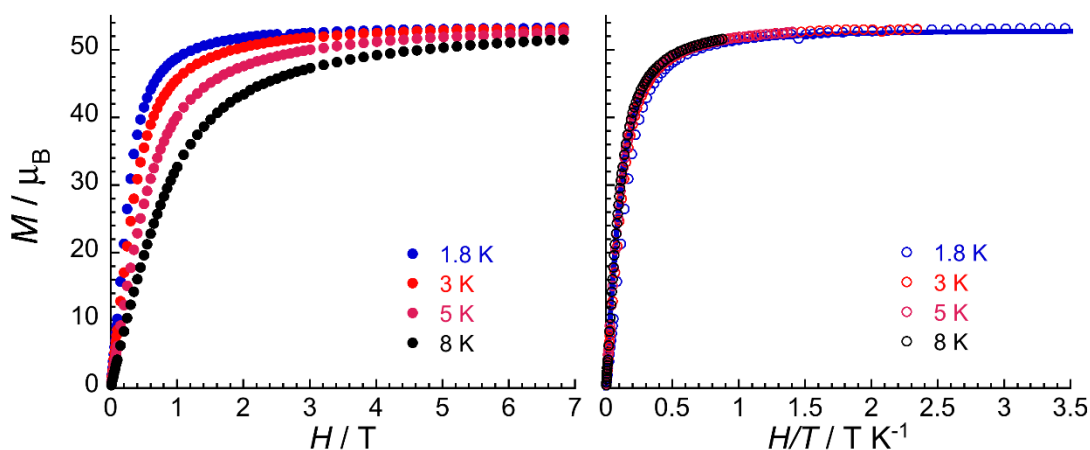
Figure 5. Field dependence of the magnetization, M, for **3** below 8 K plotted as (left) M vs H and (right) M vs H/T plots. The solid blue line is the best fit of the M vs H/T plots to a sum of the $S = 12$ and $S = 29/2$ Brillouin functions (with $g = 1.99(2)$) as discussed in the text.

In compound **3**, the statistical disorder of Mn^{II} and Ca^{II} over the six outer heptacoordinate divalent metal sites leads to the presence of an average of one Mn^{II} per coordination cluster, which implies the following average formula: $\{Mn^{II}Ca_2Mn^{III}_6\}Ca\{Ca_3Mn^{III}_6\}$. Considering the presence of dominating ferromagnetic interactions in these two sub-units, they should have overall ground state spins $S_T = 12$ (for six $S = 2$ Mn^{III} centres in $\{Ca_3Mn^{III}_6\}$) and $S_T' = 29/2$ (for six $S = 2$ Mn^{III} centers plus one $S = 5/2$ Mn^{II} site in $\{Mn^{II}Ca_2Mn^{III}_6\}$). In this hypothesis, the theoretical χT value at low temperature should then be 190.4 cm^3 K mol^{-1} (taking $g_{av} = 2$), which is in very good agreement with the experimental maximum value for χT (192 cm^3 K mol^{-1}) at 17 K. The field dependence of the magnetisation below 8 K (figure 5) shows full saturation in fields over 2 T, reaching 53.3 μ_B, again in excellent agreement with the magnetization expected for the sum of the magnetic moments for $S_T = 12$ and $S_T' = 29/2$ units (53 μ_B). The marked saturation indicates the general absence of magnetic anisotropy in this system, and that the two high-spin units each have well-defined ground states. This is further confirmed by M vs. H/T plots in which the data below 8 K are all superposed on a single master-curve, and could be fitted well by a sum of two Brillouin functions (for $S_T = 12$ and $S_T' = 29/2$ spins with an average g value of 1.99(1)). This observation

suggests that the effects of the intrinsic Mn^{III} magnetic anisotropy cannot explain the drop of the χT product below 17 K. On the other hand, the derivative of the M vs. H data shows a clear maximum at 1340 Oe at 1.85 K, which is characteristic of small antiferromagnetic interactions, in this coordination cluster most likely through the central Ca^{2+} center between the $S_T' = 29/2$ $\{Mn^{II}Ca_2Mn^{III}_6\}$ and $S_T = 12$ $\{Ca_3Mn^{III}_6\}$ units. As previously observed for the Mn_9-M-Mn_9 systems, this intra-cluster magnetic interaction can be estimated by equalisation of the Zeeman and exchange energy ($J'/k_B = g_{av}\mu_B H^*/4S_T'$), giving a value of -30(5) mK. It is interesting to note that even if most of the Mn^{II} centres have been substituted by diamagnetic Ca^{2+} in **3**, once again the effects of a weak antiferromagnetic interaction between the residual high-spin $\{Mn^{II}Ca_2Mn^{III}_6\}$ and $\{Ca_3Mn^{III}_6\}$ sub-units, mediated by the central Ca^{2+}, are observed. However, since this coupling value falls in the typical range of the dipolar interactions, it cannot be completely excluded that inter-cluster interactions could also be present and contribute phenomenologically to this value. Weak antiferromagnetic interactions are thus most likely the cause of the decrease of the χT product below 17 K.

Although complete replacement of the outer Mn^{II} ions by diamagnetic Ca^{2+} could not be achieved, it is still possible to use compound **3** as a model compound to evaluate the magnetic behaviour of the two $\{Mn^{II}Mn^{III}_6\}$ and $\{Mn^{III}_6\}$ sub-units within the structure of **1**. Based on the structure of the compound, the magnetic susceptibility was modelled as the sum of two isolated moieties, one with six $S = 2$ Mn^{III} arranged in an octahedron $\{Mn^{III}_6\}$, and the second with the same $\{Mn^{III}_6\}$ octahedron mono-capped by a Mn^{II} $S = 5/2$ ion. Only the data from above 17 K were fitted, to avoid any complications arising from interactions between the two sub-units. Furthermore, as a first approximation, only one isotropic magnetic interaction (J) was used for both the Mn^{III}-Mn^{III} and Mn^{III}-Mn^{II} interactions. The use of a single J value is justifiable since the susceptibility is largely dominated by the twelve $S = 2$ Mn^{III} ions and the ferromagnetic interactions between them, so that including the three Mn^{III}-Mn^{II} interactions

into J should not perturb it significantly from the mean $J(\text{Mn}^{III}\text{-Mn}^{III})$ value. Therefore, the magnetic susceptibility was calculated with Magpack[53] for each sub-unit according to the following Heisenberg spin Hamiltonians:

$$H = -2J\left((S_1+S_2)\bullet(S_3+S_4+S_5+S_6)+S_3\bullet S_4+S_4\bullet S_5+S_5\bullet S_6+S_3\bullet S_6\right)$$
$$H = -2J\left((S_1+S_2)\bullet(S_3+S_4+S_5+S_6)+S_3\bullet S_4+S_4\bullet S_5+S_5\bullet S_6+S_3\bullet S_6+S_7\bullet(S_1+S_4+S_5)\right)$$

Here S_i are the spin operators for each metal ion spins ($S_i = 2$ for Mn^{III} with $i = 1\text{-}6$ and $S_7 = 5/2$ for Mn^{II}). The simulation with $J/k_B = +6.0(5)$ K and $g = 2.00(5)$ is able to reproduce extremely well the experimental data above 17 K confirming the presence of two different S_T' = 29/2 $\{\text{Mn}^{II}\text{Ca}_2\text{Mn}^{III}_6\}$ and $S_T = 12$ $\{\text{Ca}_3\text{Mn}^{III}_6\}$ subunits within the molecular structure of **3**. The value of J obtained from this simulation can be compared with the average $J(\text{Mn}^{III}\text{-Mn}^{III})$ coupling constants calculated for the $[\text{Mn}_{19}]$ compound **1** of $+7.8$ and $+11.6$ K, using the B3LYP and PBE/Siesta functionals, respectively, and is in good agreement with the B3LYP value.[54] The ac susceptibility of **3** was also measured but showed no out-of-phase signal above 1.85 K and no frequency dependence of the in-phase component.

4. Conclusions

We have synthesised and structurally characterised two Mn/Ca coordination coordination clusters, a $[\text{Mn}_3\text{Ca}_3]$ compound (**2**) consistent with stoichiometric ratio of Mn/Ca employed (1:1) in the reaction and a $[\text{Mn}_{13}\text{Ca}_6]$ compound (**3**) derived from a Mn/Ca 2:1 ratio. Compound **2** presents a unique topological composition: an equilateral $\{\text{Mn}^{III}_3\}$ triangle inscribed within a triangular $\{\text{Ca}^{II}_3\}$ shell. In compound **3**, six of the seven Mn^{II} centres in the previously reported $[\text{Mn}_{19}]$ aggregate **1** have been replaced by Ca^{2+} ions, but with remarkable retention of the core topology of the parent cluster, quite close to our theoretical prediction of replacing all the Mn^{II} centres in **1** with Ca^{II} by matching their geometric and charge requirements within the $[\text{Mn}_{19}]$ system. This chemical substitution has enabled the evaluation

of the magnetism of the $\{Mn^{III}_6\}$ octahedra inscribed within the core of vertex-sharing supertetrahedron found in the $[Mn_{19}]$ system. Compound **2** lends itself to further elaboration. The magnetic properties of the Mn^{III}_3 unit could be tuned by incorporating other heterometals in place of the diamagnetic Ca^{II}. The labile terminal H_2O ligands coordinated to both Mn and Ca centres provide an opportunity to assemble the discrete molecular unit **2** into extended networks through exchange of these terminal ligands by judiciously selected bridging moieties. The development of routes for the syntheses of such species is of great importance because these systems have potential fields of applications, such as bioinorganic chemistry, magnetochemistry, materials science, and solid-state physics.

Appendix A. Supplementary data

CCDC 1044932 and 866698 contains the supplementary crystallographic data for **2** and **3**, respectively. These data can be obtained free of charge via http://www.ccdc.cam.ac.uk/conts/retrieving.html, or from the Cambridge Crystallographic Data Centre, 12 Union Road, Cambridge CB2 1EZ, UK; fax: (+44) 1223-336-033; or e-mail: deposit@ccdc.cam.ac.uk

5. References

[1] K.N. Ferreira, T.M. Iverson, K. Maghlaoui, J. Barber, S. Iwata, Architecture of the Photosynthetic Oxygen-Evolving Center, Science, 303 (2004) 1831-1838.

[2] T. Carrell, A. Tyryshkin, G. Dismukes, An evaluation of structural models for the photosynthetic water-oxidizing complex derived from spectroscopic and X-ray diffraction signatures, JBIC Journal of Biological Inorganic Chemistry, 7 (2002) 2-22.

[3] C.S. Mullins, V.L. Pecoraro, Reflections on small molecule manganese models that seek to mimic photosynthetic water oxidation chemistry, Coordination Chemistry Reviews, 252 (2008) 416-443.

[4] G. Christou, Manganese carboxylate chemistry and its biological relevance, Accounts of Chemical Research, 22 (1989) 328-335.

[5] R. Sessoli, D. Gatteschi, A. Caneschi, M.A. Novak, Magnetic bistability in a metal-ion cluster, Nature, 365 (1993) 141-143.

[6] G. Aromí, E.K. Brechin, Synthesis of 3d Metallic Single-Molecule Magnets, in: R. Winpenny (Ed.) Single-Molecule Magnets and Related Phenomena, Springer, Berlin and Heidelberg, 2006, pp. 1-67.

[7] G.E. Kostakis, A.M. Ako, A.K. Powell, Structural motifs and topological representation of Mn coordination clusters, Chemical Society Reviews, 39 (2010) 2238-2271.

[8] A. Zouni, H.-T. Witt, J. Kern, P. Fromme, N. Krauss, W. Saenger, P. Orth, Crystal structure of photosystem II from Synechococcus elongatus at 3.8 Å resolution, Nature, 409 (2001) 739-743.

[9] S.H. Kim, W. Gregor, J.M. Peloquin, M. Brynda, R.D. Britt, Investigation of the Calcium-Binding Site of the Oxygen Evolving Complex of Photosystem II Using ^{87}Sr ESEEM Spectroscopy, Journal of the American Chemical Society, 126 (2004) 7228-7237.

[10] B. Loll, J. Kern, W. Saenger, A. Zouni, J. Biesiadka, Towards complete cofactor arrangement in the 3.0 Å resolution structure of photosystem II, Nature, 438 (2005) 1040-1044.

[11] A. Boussac, F. Rappaport, P. Carrier, J.-M. Verbavatz, R. Gobin, D. Kirilovsky, A.W. Rutherford, M. Sugiura, Biosynthetic Ca^{2+}/Sr^{2+} Exchange in the Photosystem II Oxygen-evolving Enzyme of Thermosynechococcus elongatus, Journal of Biological Chemistry, 279 (2004) 22809-22819.

[12] I.J. Hewitt, J.-K. Tang, N.T. Madhu, R. Clérac, G. Buth, C.E. Anson, A.K. Powell, A series of new structural models for the OEC in photosystem II, Chemical Communications, (2006) 2650-2652.

[13] A. Mishra, W. Wernsdorfer, K.A. Abboud, G. Christou, The first high oxidation state manganese–calcium cluster: relevance to the water oxidizing complex of photosynthesis, Chemical Communications, (2005) 54-56.

[14] E.S. Koumousi, S. Mukherjee, C.M. Beavers, S.J. Teat, G. Christou, T.C. Stamatatos, Towards models of the oxygen-evolving complex (OEC) of photosystem II: a Mn_4Ca cluster of relevance to low oxidation states of the OEC, Chemical Communications, 47 (2011) 11128-11130.

[15] S. Mukherjee, J.A. Stull, J. Yano, T.C. Stamatatos, K. Pringouri, T.A. Stich, K.A. Abboud, R.D. Britt, V.K. Yachandra, G. Christou, Synthetic model of the asymmetric [Mn_3CaO_4] cubane core of the oxygen-evolving complex of photosystem II, Proceedings of the National Academy of Sciences, 109 (2012) 2257-2262.

[16] J.S. Kanady, E.Y. Tsui, M.W. Day, T. Agapie, A Synthetic Model of the Mn_3Ca Subsite of the Oxygen-Evolving Complex in Photosystem II, Science, 333 (2011) 733-736.

[17] C. Zhang, C. Chen, H. Dong, J.-R. Shen, H. Dau, J. Zhao, A synthetic Mn_4Ca-cluster mimicking the oxygen-evolving center of photosynthesis, Science, 348 (2015) 690-693.

[18] K. Olesen, L.-E. Andréasson, The Function of the Chloride Ion in Photosynthetic Oxygen Evolution, Biochemistry, 42 (2003) 2025-2035

[19] J.P. McEvoy, G.W. Brudvig, Water-Splitting Chemistry of Photosystem II, Chemical Reviews, 106 (2006) 4455-4483 (see particularly Refs. 93-115)

[20] A.M. Ako, I.J. Hewitt, V. Mereacre, R. Clérac, W. Wernsdorfer, C.E. Anson, A.K. Powell, A Ferromagnetically Coupled Mn_{19} Aggregate with a Record S=83/2 Ground Spin State, Angewandte Chemie International Edition, 45 (2006) 4926-4929.

[21] A.M. Ako, M.S. Alam, S. Mameri, Y. Lan, M. Hibert, M. Stocker, P. Müller, C.E. Anson, A.K. Powell, Adsorption of [Mn_{19}] Aggregates with S = 83/2 onto HOPG Surfaces, European Journal of Inorganic Chemistry, (2012) 4131-4140.

[22] S. Mameri, A.M. Ako, F. Yesil, M. Hibert, Y. Lan, C.E. Anson, A.K. Powell, Coordination Cluster Analogues of the High-Spin [Mn_{19}] System with Functionalized 2,6-Bis(hydroxymethyl)phenol Ligands, European Journal of Inorganic Chemistry, 2014 (2014) 4326-4334.

[23] A.M. Ako, Y. Lan, O. Hampe, E. Cremades, E. Ruiz, C.E. Anson, A.K. Powell, All-round robustness of the Mn_{19} coordination cluster system: experimental validation of a theoretical prediction, Chemical Communications, 50 (2014) 5847-5850.

[24] A.M. Ako, V. Mereacre, R. Clérac, W. Wernsdorfer, I.J. Hewitt, C.E. Anson, A.K. Powell, A [$Mn_{18}Dy$] SMM resulting from the targeted replacement of the central Mn^{II} in the S = 83/2 [Mn_{19}]-aggregate with Dy^{III}, Chemical Communications, (2009) 544-546.

[25] A.M. Ako, B. Burger, Y. Lan, V. Mereacre, R. Clérac, G. Buth, S. Gómez-Coca, E. Ruiz, C.E. Anson, A.K. Powell, Magnetic Interactions Mediated by Diamagnetic Cations in [$Mn_{18}M$] (M = Sr^{2+}, Y^{3+}, Cd^{2+}, and Lu^{3+}) Coordination Clusters, Inorganic Chemistry, 52 (2013) 5764-5774.

[26] T. Glaser, I. Liratzis, A.M. Ako, A.K. Powell, 2,6-Bis(hydroxymethyl)phenols for the synthesis of high-nuclearity clusters, Coordination Chemistry Reviews, 253 (2009) 2296-2305.

[27] G. Sheldrick, A short history of SHELX, Acta Crystallographica Section A, 64 (2008) 112-122.

[28] G. Sheldrick, Crystal structure refinement with SHELXL, Acta Crystallographica Section C, 71 (2015) 3-8.

[29] A. Spek, PLATON SQUEEZE: a tool for the calculation of the disordered solvent contribution to the calculated structure factors, Acta Crystallographica Section C, 71 (2015) 9-18.

[30] R. Shannon, Revised effective ionic radii and systematic studies of interatomic distances in halides and chalcogenides, Acta Crystallographica Section A, 32 (1976) 751-767.

[31] W. Liu, H.H. Thorp, Bond valence sum analysis of metal-ligand bond lengths in metalloenzymes and model complexes. 2. Refined distances and other enzymes, Inorganic Chemistry, 32 (1993) 4102-4105.

[32] E.M. Sproviero, J.A. Gascón, J.P. McEvoy, G.W. Brudvig, V.S. Batista, Computational studies of the O_2-evolving complex of photosystem II and biomimetic oxomanganese complexes, Coordination Chemistry Reviews, 252 (2008) 395-415.

[33] P.E.M. Siegbahn, Structures and Energetics for O_2 Formation in Photosystem II, Accounts of Chemical Research, 42 (2009) 1871-1880.

[34] S. Petrie, R. Stranger, R.J. Pace, Location of Potential Substrate Water Binding Sites in the Water Oxidizing Complex of Photosystem II, Angewandte Chemie International Edition, 49 (2010) 4233-4236.

[35] Y.J. Park, J.W. Ziller, A.S. Borovik, The Effects of Redox-Inactive Metal Ions on the Activation of Dioxygen: Isolation and Characterization of a Heterobimetallic Complex Containing a Mn^{III}–(μ-OH)–Ca^{II} Core, Journal of the American Chemical Society, 133 (2011) 9258-9261.

[36] R. Inglis, C.J. Milios, L.F. Jones, S. Piligkos, E.K. Brechin, Twisted molecular magnets, Chemical Communications, 48 (2012) 181-190.

[37] A.M. Mowson, T.N. Nguyen, K.A. Abboud, G. Christou, Dimeric and Tetrameric Supramolecular Aggregates of Single-Molecule Magnets via Carboxylate Substitution, Inorganic Chemistry, 52 (2013) 12320-12322.

[38] T.N. Nguyen, W. Wernsdorfer, K.A. Abboud, G. Christou, A Supramolecular Aggregate of Four Exchange-Biased Single-Molecule Magnets, Journal of the American Chemical Society, 133 (2011) 20688-20691.

[39] G.M. Dulcevscaia, I.G. Filippova, M. Speldrich, J. van Leusen, V.C. Kravtsov, S.G. Baca, P. Kögerler, S.-X. Liu, S. Decurtins, Cluster-Based Networks: 1D and 2D Coordination Polymers Based on {$MnFe_2(\mu_3$-O)}-Type Clusters, Inorganic Chemistry, 51 (2012) 5110-5117.

[40] T. Weyhermüller, R. Wagner, S. Khanra, P. Chaudhuri, A magnetostructural study of linear $Ni^{II}Mn^{III}Ni^{II}$, $Ni^{II}Cr^{III}Ni^{II}$ and triangular Ni^{II}_3 species containing (pyridine-2-aldoximato)nickel(II) unit as a building block, Dalton Transactions, (2005) 2539-2546.

[41] X. Bao, W. Liu, J.-L. Liu, S. Gómez-Coca, E. Ruiz, M.-L. Tong, Self-Assembly of Pentanuclear Mesocate versus Octanuclear Helicate: Size Effect of the $[M^{II}_3(\mu_3\text{-O/X})]^{n+}$ Triangle Core, Inorganic Chemistry, 52 (2013) 1099-1107.

[42] C. Lampropoulos, K.A. Abboud, T.C. Stamatatos, G. Christou, A Nontwisted, Ferromagnetically Coupled Mn^{III}_3O Triangular Complex from the Use of 2,6-Bis(hydroxymethyl)-p-cresol, Inorganic Chemistry, 48 (2009) 813-815.

[43] S.G. Sreerama, S. Pal, A Novel Carboxylate-Free Ferromagnetic Trinuclear μ_3-Oxo–Manganese(III) Complex with Distorted Pentagonal-Bipyramidal Metal Centers, Inorganic Chemistry, 41 (2002) 4843-4845.

[44] M. Li, Y. Lan, A.M. Ako, W. Wernsdorfer, C.E. Anson, G. Buth, A.K. Powell, Z. Wang, S. Gao, A Family of 3d-4f Octa-Nuclear $[Mn^{III}_4Ln^{III}_4]$ Wheels (Ln = Sm, Gd, Tb, Dy, Ho, Er, and Y): Synthesis, Structure, and Magnetism, Inorganic Chemistry, 49 (2010) 11587-11594.

[45] F.K. Larsen, E.J.L. McInnes, H.E. Mkami, J. Overgaard, S. Piligkos, G. Rajaraman, E. Rentschler, A.A. Smith, G.M. Smith, V. Boote, M. Jennings, G.A. Timco, R.E.P. Winpenny, Synthesis and Characterization of Heterometallic $\{Cr_7M\}$ Wheels, Angewandte Chemie International Edition, 42 (2003) 101-105.

[46] R.W. Saalfrank, R. Prakash, H. Maid, F. Hampel, F.W. Heinemann, A.X. Trautwein, L.H. Böttger, Synthesis and Characterization of Metal-Centered, Six-Membered, Mixed-Valent, Heterometallic Wheels of Iron, Manganese, and Indium, Chemistry – A European Journal, 12 (2006) 2428-2433.

[47] C.-F. Lee, D.A. Leigh, R.G. Pritchard, D. Schultz, S.J. Teat, G.A. Timco, R.E.P. Winpenny, Hybrid organic–inorganic rotaxanes and molecular shuttles, Nature, 458 (2009) 314-318.

[48] E.C. Sañudo, C.A. Muryn, M.A. Helliwell, G.A. Timco, W. Wernsdorfer, R.E.P. Winpenny, Al, Ga and In heterometallic wheels and their by-products, Chemical Communications, (2007) 801-803.

[49] Y. Chen-I, T. Hui-Lien, L. Gene-Hsiang, W. Ching-Shuei, Y. Shwu-Fen, A Mixed-metal Single-molecule Magnet: $[Mn_8Fe_4O_{12}(O_2CCH_2Cl)_{16}(H_2O)_4]$, Chemistry Letters, 34 (2005) 288-289.

[50] J.H. Van Vleck, The theory of electric and magnetic susceptibilities, Repr. ed., Oxford : Oxford university press, 1965.

[51] K. Kambe, On the Paramagnetic Susceptibilities of Some Polynuclear Complex Salts, Journal of the Physical Society of Japan, 5 (1950) 48-51.

[52] J. Tang, I. Hewitt, N.T. Madhu, G. Chastanet, W. Wernsdorfer, C.E. Anson, C. Benelli, R. Sessoli, A.K. Powell, Dysprosium Triangles Showing Single-Molecule Magnet Behavior of Thermally Excited Spin States, Angewandte Chemie International Edition, 45 (2006) 1729-1733.

[53] J.J. Borrás-Almenar, J.M. Clemente-Juan, Coronado, E., B.S. Tsukerblat, MAGPACK A package to calculate the energy levels, bulk magnetic properties, and inelastic neutron scattering spectra of high nuclearity spin clusters, Journal of Computational Chemistry, 22 (2001) 985-991.

[54] E. Ruiz, T. Cauchy, J. Cano, R. Costa, J. Tercero, S. Alvarez, Magnetic Structure of the Large-Spin Mn_{10} and Mn_{19} Complexes: A Theoretical Complement to an Experimental Milestone, Journal of the American Chemical Society, 130 (2008) 7420-7426.